Egyptian Journal of Aquatic Biology & Fisheries
Zoology Department, Faculty of Science,
Ain Shams University, Cairo, Egypt.
ISSN 1110 – 6131
Vol. 29(5): 2103 – 2122 (2025)
www.ejabf.journals.ekb.eg


# Highly Selective and Sensitive Photoluminescent Detection of Lornoxicam in River Nile and Pharmaceutical Samples

**Mohamed E. Negm[1], Ahmed O. Youssef[1], M. Kenawy[1], Maged El-Kemary[2], Mohamed S. Attia[1*]**

[1]Chemistry Department, Faculty of Science, Ain Shams University, Abbassia, Cairo, 11566, Egypt
[2]Nano Science and Technology Institute, Kafrelsheikh University, Kafrelsheikh, Egypt
[*]**Corresponding Author: mohd_mostafa@sci.asu.edu.eg**

## ARTICLE INFO

**Article History:**
Received: Aug. 26, 2025
Accepted: Sep. 27, 2025
Online: Oct. 10, 2025

**Keywords**:
Photoprobe,
Lornoxicam,
Cavity,
Fluorescence,
Enhancement

## ABSTRACT

This study introduces a novel, highly sensitive method for detecting Lornoxicam (LORN) based on its complexation with terbium (Tb) ions. The Tb-LORN complex exhibits unique photoluminescent properties, where energy absorbed by LORN at 270nm is transferred to $Tb^{3+}$, resulting in a characteristic emission at 545nm. This specific energy transfer enables the selective quantification of LORN over a wide linear range ($5 \times 10^{-9}$ to $5 \times 10^{-5}$ mol/L). The method was successfully applied to determine LORN concentrations in pharmaceutical formulations and environmental samples, specifically industrial wastewater from the Nile River region, demonstrating its practical utility for quality control and environmental monitoring.

## INTRODUCTION

Lornoxicam (chemically defined as 6-Chloro-4-hydroxy-2-methyl-N-2-pyridinyl-2H-thieno[2,3-e]-1,2-thiazine-3-carboxamide 1,1-dioxide) is a member of the oxicam class of non-steroidal anti-inflammatory drugs (NSAIDs). As illustrated in Fig. (1), it possesses significant analgesic and antipyretic properties, making it effective for managing pain associated with conditions like osteoarthritis, rheumatoid arthritis, and acute lower back pain **(Balfour *et al.*, 1996)**.

The therapeutic action of lornoxicam stems from its potent inhibition of cyclooxygenase (COX) enzymes. These enzymes are key in synthesizing prostaglandins from arachidonic acid; prostaglandins are messenger molecules that mediate inflammation, pain, and fever. By suppressing their production, lornoxicam effectively reduces these symptoms **(Balfour *et al.*, 1996)**. A distinctive feature of lornoxicam compared to other oxicams is its relatively short elimination half-life, which is believed to contribute to a more favorable tolerability profile **(Balfour *et al.*, 1996)**. Given its widespread use as a potent analgesic, there is a clear need for accurate, sensitive, and

straightforward analytical methods to quantify it in pharmaceuticals and environmental samples.

Several techniques have been employed for lornoxicam determination. For instance, one study used high-performance liquid chromatography–tandem mass spectrometry (HPLC-MS/MS), but this method required a large plasma volume (0.5mL) and had a limited quantification sensitivity of 2.0ng/ mL **(Chaplenko *et al.*, 2018)**. Other approaches, such as UV spectrophotometry, can be susceptible to electronic noise and interference **(Taha *et al.*, 2006)**, while voltammetric methods using carbon electrodes may be slow and suffer from matrix effects **(Ghoneim *et al.*, 2002; Bozal & Uslu, 2010; Sahoo *et al.*, 2012; Salunkhe *et al.*, 2019; Belal *et al.*, 2020)**. In contrast, luminescent sensors based on lanthanide complexes offer notable advantages, including high stability and a long operational lifetime—often maintaining a constant signal for up to two years. They also typically provide low standard deviations due to fewer potential sources of error during measurement **(Zhang *et al.*, 2003; Weibel *et al.*, 2004; Hanaoka *et al.*, 2007; Escudero *et al.*, 2017)**. This work introduces a novel fluorescent optical sensor for the selective detection of lornoxicam. The proposed method utilizes a $Tb^{3+}$ (terbium) chemosensor operating at pH 5.5 and is applied to the analysis of pharmaceutical formulations and the Nile River water samples.

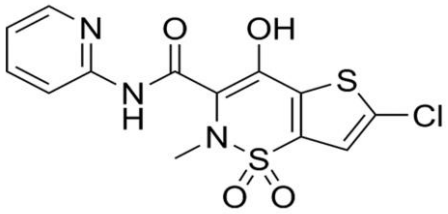


**Fig. 1.** Structure of lornoxicam

## MATERIALS AND METHODS

### 1. Materials and reagents

All chemicals utilized were of analytical grade or higher purity. A stock solution of Lornoxicam (LORN) was prepared in acetonitrile and subsequently diluted to yield a working concentration of $1.0 \times 10^{-4}$ mol/L. Vials of a pharmaceutical formulation (Global Napi Co., Egypt) containing 8mg of lornoxicam per 2ml were procured from a local pharmacy. A $1.0 \times 10^{-2}$ mol/L stock solution of $Tb^{3+}$ ions was produced by dissolving $Tb(NO_3)_3$ (Aldrich, 99.99%) in ethanol within a 25ml volumetric flask. This stock solution was then diluted with ethanol to create a fresh working solution of $Tb^{3+}$ at $1.0 \times 10^{-4}$ mol/L.

## 2. Instrumentation

Luminescence measurements were conducted using an FS5 spectrofluorometer (Edinburgh Instruments), which features high-resolution monochromators and sensitive, rapid data collection capabilities. Absorption spectra were acquired with a DS5 UV-Vis spectrophotometer, equipped with Tungsten-Halogen and Deuterium light sources and a silicon photodiode detector. pH measurements were performed with an ORION model 290A pH meter.

## 3. General analytical procedure

The experimental protocol involved combining 0.1ml aliquots of both the $1.0 \times 10^{-2}$ mol/L LORN solution and the $1.0 \times 10^{-2}$ mol/L $Tb^{3+}$ solution in a 10ml volumetric flask. The mixture was diluted to volume with acetonitrile and was allowed to stand for 15 minutes prior to analysis. This prepared sensor solution was used to record absorption and emission spectra, investigate the influence of pH and different solvents, and measure luminescence intensity at an excitation/emission wavelength pair of 270 and 545nm.

## 4. Construction of the calibration curve

A calibration curve was generated by reacting the $Tb^{3+}$ solution with a series of LORN standards covering a concentration range from $5.0 \times 10^{-4}$ mol/L to $1.0 \times 10^{-9}$ mol/L. These standards were prepared in 10mL volumetric flasks from the original stock solution. The luminescence intensity of each standard was measured at an excitation wavelength (λ_ex) of 270nm. The spectrofluorometer cell was thoroughly rinsed with acetonitrile between each measurement to prevent cross-contamination.

## 5. Method of detecting lornoxicam in a real sample from industrial waste on the Nile River

The method is based on forming a luminescent complex between lornoxicam (LORN) and terbium ions ($Tb^{3+}$). Lornoxicam itself may have weak luminescence, but when it binds to $Tb^{3+}$, it acts as an "antenna," absorbing light and efficiently transferring the energy to the $Tb^{3+}$ ion. This causes the $Tb^{3+}$ ion to emit its own characteristic, strong luminescence at 545nm. The intensity of this light is directly proportional to the concentration of lornoxicam in the sample, allowing for its quantification.

### Step 1: Sample collection and pre-treatment

Water samples were collected from the suspected industrial waste discharge point into the River Nile using clean glass bottles. The samples were filtered immediately, or upon returning to the laboratory, to remove suspended solids, algae, and other particulate matter that could interfere with the analysis. A standard filter paper or a 0.45µm

membrane filter was used.

Because the concentration of lornoxicam in river water was expected to be very low (trace levels), a pre-concentration step was carried out before analysis. Liquid–Liquid Extraction (LLE) was employed for this purpose. The filtered water samples were shaken with a smaller volume of an organic solvent such as dichloromethane or ethyl acetate. Lornoxicam, being organic, partitioned from the aqueous phase into the organic phase.

The organic layer was then separated and evaporated to dryness under a gentle stream of nitrogen or using a rotary evaporator. The dry residue was re-dissolved in a small, known volume of acetonitrile, which served as the solvent specified in the analytical method. This step both concentrated the analyte and placed it in the appropriate matrix for subsequent analysis.

**Step 2: Complex formation (Derivatization)**

A measured volume (0.1mL) of the pre-treated and concentrated sample solution in acetonitrile was transferred into a test tube. Then, 0.1mL of the working $Tb^{3+}$ solution ($1.0 \times 10^{-4}$ mol/L) was added. The mixture was transferred to a 10mL volumetric flask and diluted to the mark with acetonitrile. The solution was allowed to stand for 15 minutes to ensure complete formation of the LORN–$Tb^{3+}$ complex.

**Step 3: Instrumental measurement**

Fluorescence measurements were performed using an FS5 spectrofluorometer. The instrument was allowed to warm up prior to use. The excitation wavelength (λ_ex) was set to 270nm, and the emission intensity was measured at 545nm (λ_em), corresponding to the characteristic green emission of $Tb^{3+}$. Each sample was placed in a clean quartz cuvette for measurement, and the cuvette was rinsed thoroughly with acetonitrile after each use to prevent cross-contamination.

**Step 4: Quantification using the calibration curve**

Quantification of lornoxicam was carried out using a calibration curve prepared from standard solutions of known concentration. Following Section 2.4, a series of standard solutions of pure lornoxicam were prepared in the range of $5.0 \times 10^{-9}$ to $5.0 \times 10^{-4}$ mol/L. Each standard was treated in the same manner as the samples—mixed with $Tb^{3+}$, diluted to 10mL with acetonitrile, and incubated for 15 minutes.

The luminescence intensity of each standard solution was measured at 545nm, and a calibration curve was constructed by plotting luminescence intensity (y-axis) against lornoxicam concentration (x-axis). The resulting curve exhibited a linear relationship.

The luminescence intensity of the pre-treated waste sample was then measured under the same conditions. Its corresponding concentration was determined from the calibration curve. Finally, the concentration of lornoxicam in the original River Nile sample was calculated by accounting for all dilution and concentration factors applied during pre-treatment.

## 6. Validation

### *6.1. Accuracy and precision*

The precision of the analytical procedure was determined by testing lornoxicam samples at two concentration levels ($1.0 \times 10^{-6}$ M and $1.0 \times 10^{-7}$ M). To assess both intra-day (repeatability) and inter-day (intermediate) precisions, three repeated analyses were conducted within a single day and across three separate days, respectively. The results, detailed in Table (1) show low relative standard deviation (%RSD) values, reflecting minimal variability in the measurements. The %RSD for intra-day precision fell within a narrow range of 2.14 to 2.70%, while inter-day precision yielded values from 3.30 to 3.50%. These low %RSD figures confirm the method's excellent reproducibility. Furthermore, the method's accuracy was confirmed to be high, as determined by calculating the percentage relative error (%RE) between the measured and the expected concentrations.

### *6.2. Selectivity*

The selectivity of the method was evaluated by testing a synthetic mixture that included LORN and a placebo blank. The placebo was composed of typical excipients: 40mg of cellulose, 30mg of starch, 50mg of lactose, 200mg of povidone, 50mg of sodium starch glycolate, and 20mg of magnesium stearate. When the extracted excipients were analyzed using the proposed method, their luminescence spectra showed no overlapping signals with LORN, thereby confirming the method's selectivity. A further competitive analysis was performed on a synthetic mixture containing a known quantity of lornoxicam. This involved preparing a solution with the placebo components and the drug. After processing the mixture and filtering, the final solution contained lornoxicam at a concentration of $1.0 \times 10^{-6}$ mol/L. Analysis of this solution in triplicate resulted in a very low %RSD of 0.6% for the lornoxicam signal (Table 2), providing additional evidence of the method's high selectivity.

### *6.3. Determination of LORN in pharmaceutical preparations*

The applicability of the method for analyzing commercial pharmaceutical products was tested. Two standard Lornoxicam solutions ($1.0 \times 10^{-6}$ M and $1.0 \times 10^{-7}$ M) were prepared. A measured volume from an 8mg Lornoxicam vial was diluted with

acetonitrile in a 10mL volumetric flask and then complexed with $Tb^{3+}$ ($10^{-4}$ M) to form the photo-probe. The luminescence intensities of these probes were measured to validate the method's practicality. The obtained intensity readings were compared against the calibration curve generated from standard solutions of known concentration.

## RESULTS AND DISCUSSION

### 1. Spectral characteristics

### Absorption spectra

Fig. (2) compares the absorption spectra of pure lornoxicam and its complex with terbium ions ($Tb^{3+}$). The formation of a coordination bond between $Tb^{3+}$ and lornoxicam alters the molecule's electronic environment. This interaction is evidenced by a blue-shift (a shift to shorter wavelengths) in the characteristic absorption peaks of lornoxicam from 270, 290, and 385 nm to 263, 282, and 377 nm, respectively. The peak at 230nm remains unchanged. This hypsochromic shift indicates that the complex requires higher energy for electronic transitions, likely due to electron withdrawal by the terbium ion. Furthermore, the intense quenching of fluorescence suggests an efficient energy transfer from the excited lornoxicam to the $Tb^{3+}$ ion. Such spectral shifts are a recognized indicator of complex formation between lanthanide ions like terbium and organic ligands.

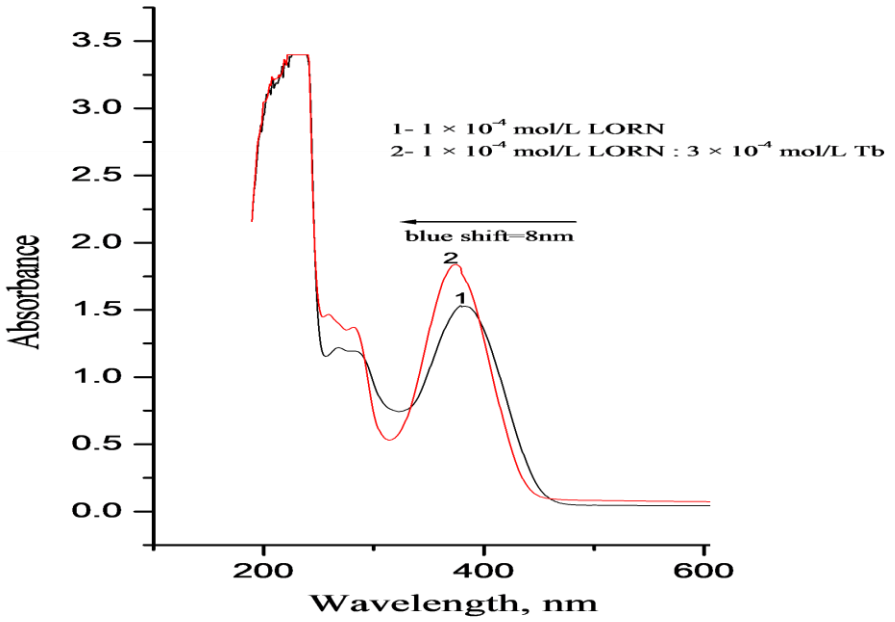


**Fig. 2.** Absorption spectra of (1) $1\times10^{-4}$ M of (lornoxicam) in acetonitrile and (2) $1\times10^{-4}$ M of (lornoxicam) in the presence of $3\times10^{-4}$ M of $Tb^{3+}$ in acetonitrile

## 2. Effect of molar ratio on the luminescence spectrum

The luminescence intensity of the Tb-lornoxicam complex increases with a higher molar ratio of $Tb^{3+}$ to lornoxicam, reaching a maximum at a 1:1 ratio. This enhancement occurs because a greater availability of terbium ions promotes more efficient binding to lornoxicam via its nitrogen, oxygen, and sulfur atoms. The optimal 1:1 ratio suggests that terbium occupies multiple binding sites on each lornoxicam molecule, maximizing the energy transfer from the excited ligand to the terbium ion, which subsequently emits light through its characteristic f-f transitions upon excitation at 270 nm.

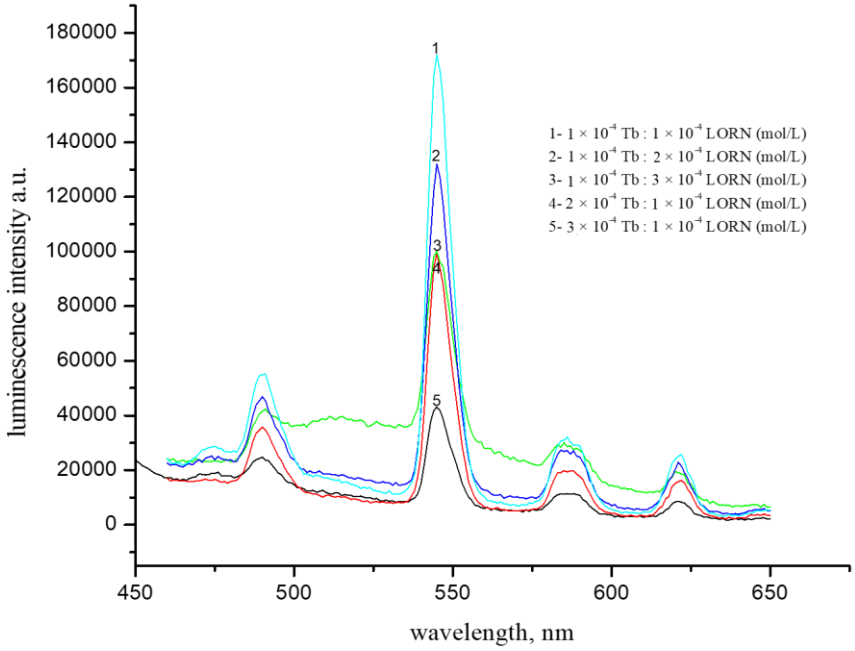


**Fig. 3.** Luminescence spectra of different Molar ratios between $Tb^{3+}$ and lornoxicam in acetonitrile at $\lambda_{ex}$=270 nm

## 3. Effect of solvent on luminescence spectrum

The superior luminescence intensity of Tb-lornoxicam in acetonitrile, relative to solvents like ethanol, DMSO, DMF, and water, can be attributed to several key solvent properties. First, acetonitrile's specific polarity is optimal. Polar solvents stabilize molecular excited states by absorbing vibrational energy, which reduces the energy gap between the ground and excited states. This enhanced stabilization in acetonitrile facilitates a more efficient energy transfer from the ligand to the terbium ion following excitation at 270nm. Second, unlike protic solvents such as ethanol and water, acetonitrile engages in only weak hydrogen bonding. Since strong hydrogen bonding offers a non-

radiative pathway for de-excitation (quenching), its minimal presence in acetonitrile helps preserve luminescence. Finally, the molecular structure of acetonitrile may promote a more favorable orientation of the terbium ion for light emission **(Attia & Al-Radadi, 2016; Attia *et al.*, 2018, 2022; AlGhamdi *et al.*, 2023; Younis *et al.*, 2023)**.

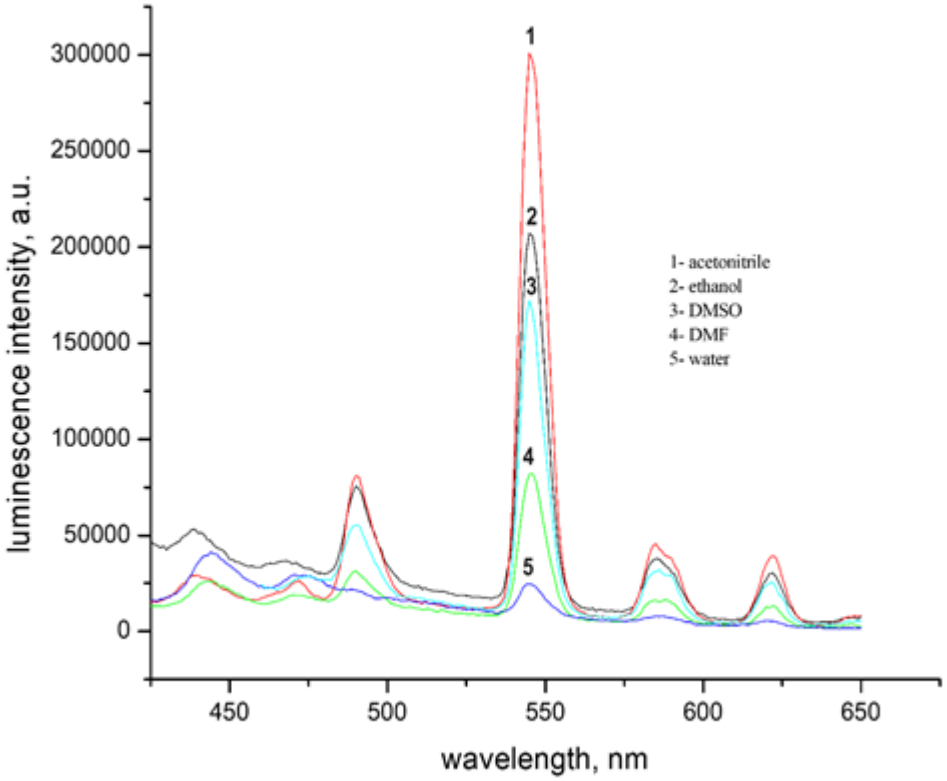


**Fig. 4.** Luminescence emission spectra of $3x10^{-4}$ mol $L^{-1}$ $Tb^{3+}$ in the presence of $1x10^{-4}$ mol/L of lornoxicam in different solvents at $\lambda_{ex}$=270 nm.

**4. pH effect on luminescence spectrum**

Fig. (5) illustrates how the luminescence intensity of the Tb(III)-lornoxicam complex in an aqueous medium changes with pH. The luminescence is most intense at pH 5.5 and 7, diminishes at pH 4 and 8, and is weakest at pH 9 and 10. This pattern is governed by the protonation state of the lornoxicam ligand and its subsequent ability to coordinate with the terbium ion.

At moderately acidic to neutral pH (5.5 and 7), the heteroatoms within lornoxicam are predominantly deprotonated. This generates negatively charged sites that strongly attract and bind the positively charged $Tb^{3+}$ ion, particularly at nitrogen and oxygen

atoms. This optimal coordination geometry leads to the highest observed luminescence intensity.

In contrast, under more acidic conditions (pH 4), these heteroatoms become protonated. This protonation reduces the ligand's negative charge and its chelating ability, resulting in weaker binding to terbium and a consequent decrease in luminescence.

Under basic conditions (pH 8 to 10), although the ligand is deprotonated, the luminescence is quenched. This is attributed to competitive binding between the deprotonated lornoxicam and hydroxide ions ($OH^-$) from the medium for the $Tb^{3+}$ ion. The formation of terbium-hydroxide species disrupts the efficient energy transfer required for strong luminescence, causing the intensity to fall **(Attia *et al.*, 2011a, b, c, 2012a, b)**.

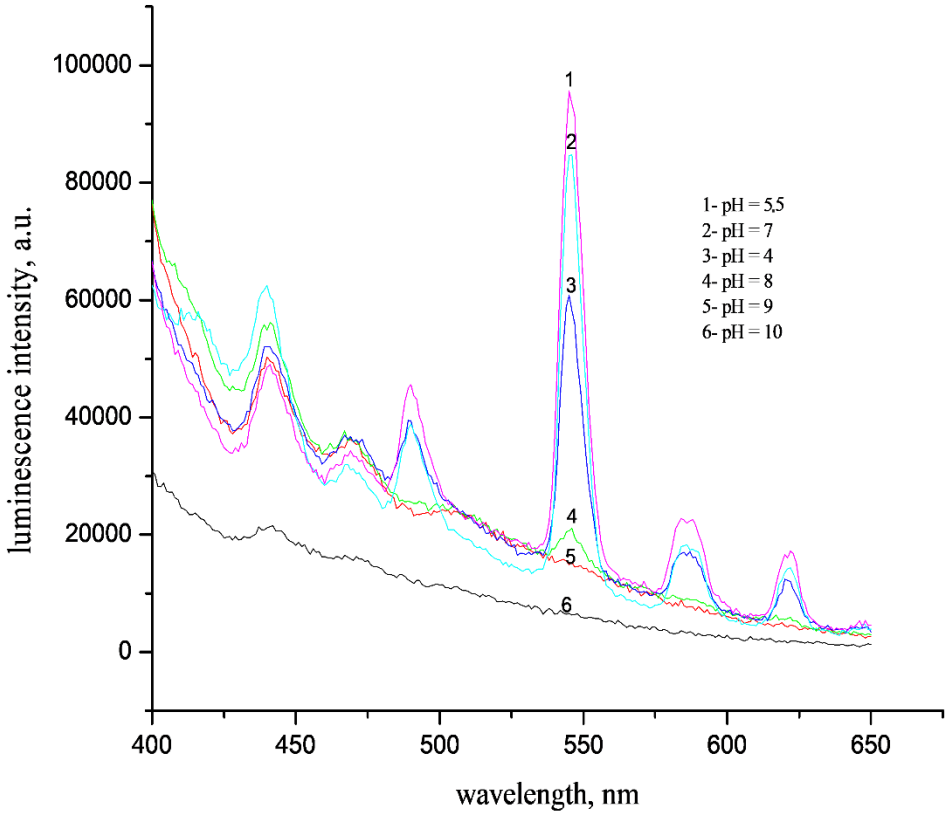


**Fig. 5.** Luminescence emission spectra of $3x10^{-4}$ mol/L of $Tb^{3+}$ in the presence of $1x10^{-4}$ mol/L lornoxicam in acetonitrile at different pH at $\lambda_{ex}$=270 nm.

## 5. Lifetime

Luminescence lifetime is a vital parameter for lanthanide complexes, with the

long-lived emission of $Tb^{3+}$ being particularly advantageous. Lasting on the order of microseconds, this extended lifetime creates a clear time-based window to separate the terbium luminescence from the rapid, auto-fluorescence of biological samples and other short-lived components. Consequently, this temporal discrimination simplifies the analysis of molecular associations and dynamic processes within a system. For the specific $Tb^{3+}$-lornoxicam complex, the decay profile in Fig. (6) shows a $^5D_4$ excited state lifetime of $5.04 \times 10^3$ μs, measured at an emission wavelength (λem) of 545nm.

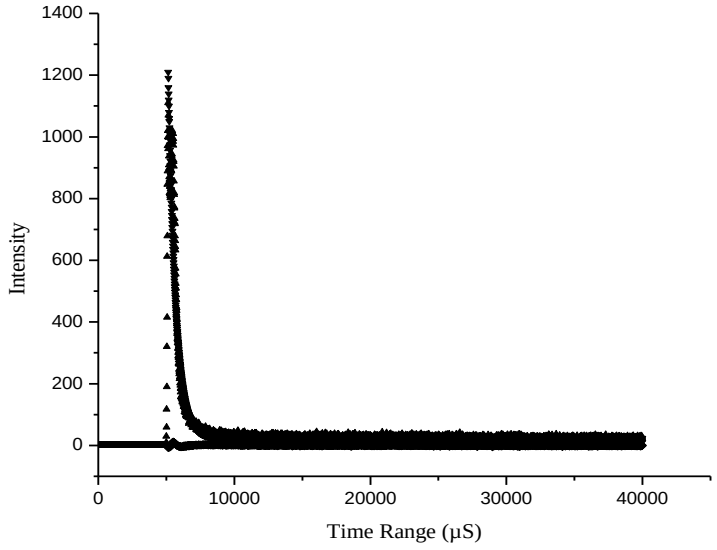


**Fig. 6.** Normalized time-resolved decay spectra of $Tb^{3+}$- lornoxicam photo probe

## 6. CIE chromaticity coordinates

Based on the data presented in Fig. (7), the CIE chromaticity coordinates for the Tb-Lornoxicam cal $5 \times 10^{-5}$ sample are estimated to be near (0.390, 0.420). In the CIE color space, the x-axis corresponds to the red component and the y-axis to the green component of the perceived color. The point is located by approximating its position where the vertical grid line for x=0.390 meets the horizontal grid line for y=0.420. This specific coordinate indicates that the compound's emission possesses a color quality with a slightly greater green intensity compared to red. The curved boundary on the diagram shows the locus of pure monochromatic colors.

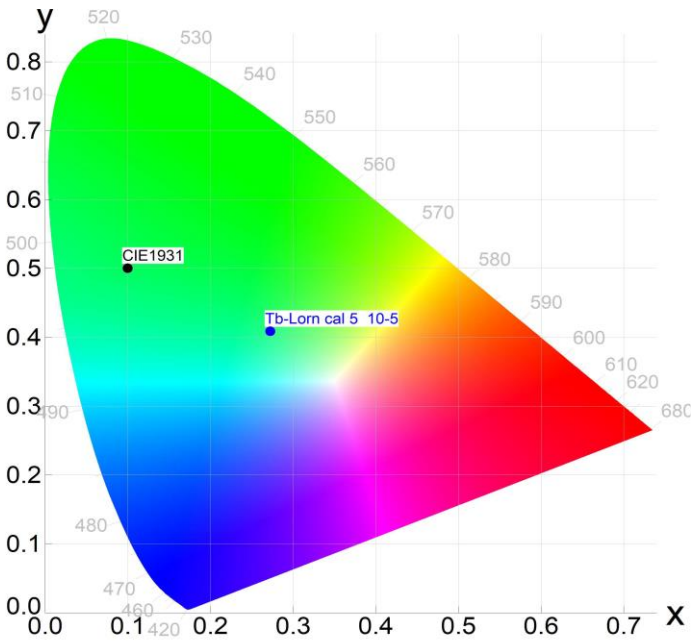


**Fig. 7.** CIE chromaticity coordinates of $Tb^{3+}$- Lornoxicam complex

## 7. Quantum yield calculations

The luminescence quantum yield (QY) is a critical photophysical parameter defined as the efficiency of a substance to emit photons upon absorption of light. It is calculated as the ratio of photons emitted to photons absorbed. For the Terbium-Lornoxicam (Tb-Lornoxicam) complex in acetonitrile, the quantum yield was determined to be 36.74% (Fig. 8).

This relatively high QY indicates an efficient conversion of absorbed ultraviolet (UV) light into visible emission. The mechanism involves the absorption of energy by the organic Lornoxicam ligand, followed by a transfer of that energy to the central terbium ion ($Tb^{3+}$). The $Tb^{3+}$ ion then releases this energy as characteristic luminescence. The efficiency of this intramolecular energy transfer is crucial and depends on the spectral overlap between the ligand's absorption and the metal ion's emission profiles.

A high quantum yield is essential for practical applications. For instance, the Tb-Lornoxicam complex shows promise for use in luminescent solar concentrators (LSCs). In such devices, a high QY ensures that a greater proportion of absorbed sunlight is successfully converted and concentrated into light that can be used more effectively by photovoltaic cells.

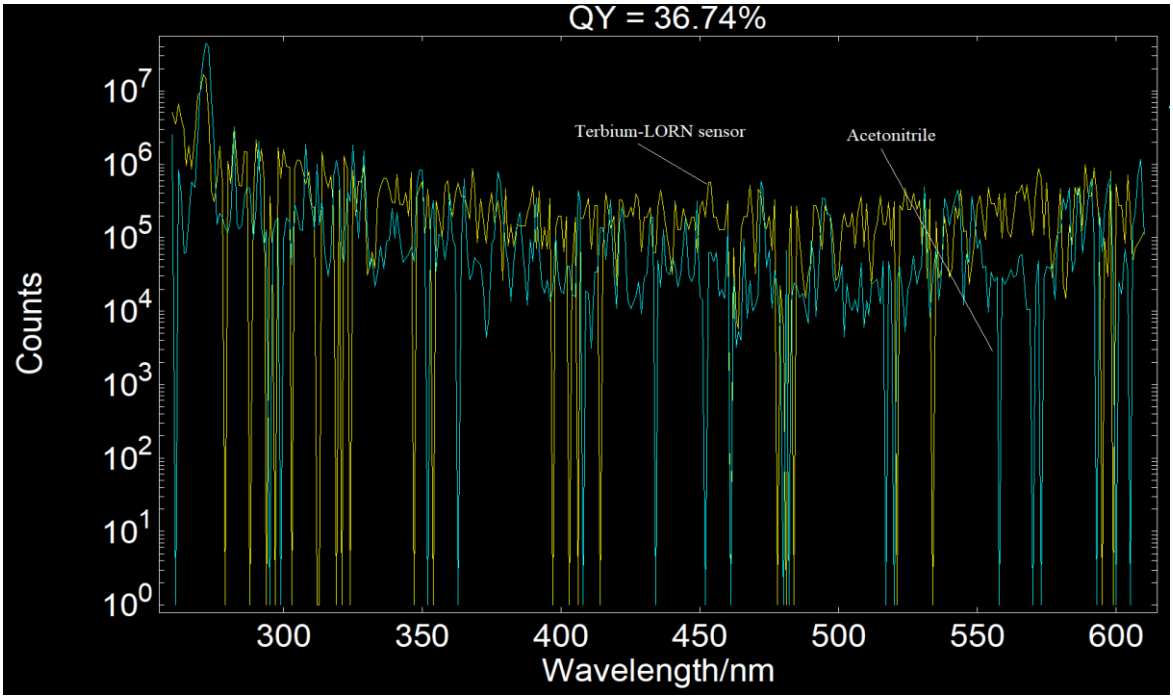


**Fig. 8.** Emission quantum yield spectra of acetonitrile and $Tb^{3+}$- Lornoxicam photo probe in acetonitrile

## 8. Method validation

### *8.1. Calibration curve*

Fig. (9) displays the emission profiles of $Tb^{3+}$ ions combined with varying amounts of lornoxicam in acetonitrile. The observed peaks correspond to specific electronic transitions within the $Tb^{3+}$ ion:

The most energetic peak, at 490nm, originates from the $^5D_4 \rightarrow {}^7F_6$ transition. This high-energy emission results from the significant energy gap between the $^5D_4$ excited state and the $^7F_6$ ground state.

The characteristic green emission at 545nm is due to the $^5D_4 \rightarrow {}^7F_5$ transition. A slightly smaller energy difference compared to the previous transition leads to this longer wavelength, green light.

A weaker, yellow emission peak is observed at 590 nm, which is assigned to the $^5D_4 \rightarrow {}^7F_4$ transition. The further reduction in the energy gap results in this lower-energy emission.

The weakest peak, appearing at 620nm in the red region, arises from the $^5D_4 \rightarrow {}^7F_3$ transition. This represents the smallest energy difference and thus the longest

wavelength emission among the four.

The intensity of these emissions is influenced by factors such as ion concentration, temperature, and the chemical environment. In this case, the consistent relative intensities across different Lornoxicam concentrations suggest that the $Tb^{3+}$ ion concentration itself is not the primary variable. Instead, the role of Lornoxicam is likely to shield the $Tb^{3+}$ ions from solvent molecules, thereby reducing quenching and enhancing the overall luminescence intensity.

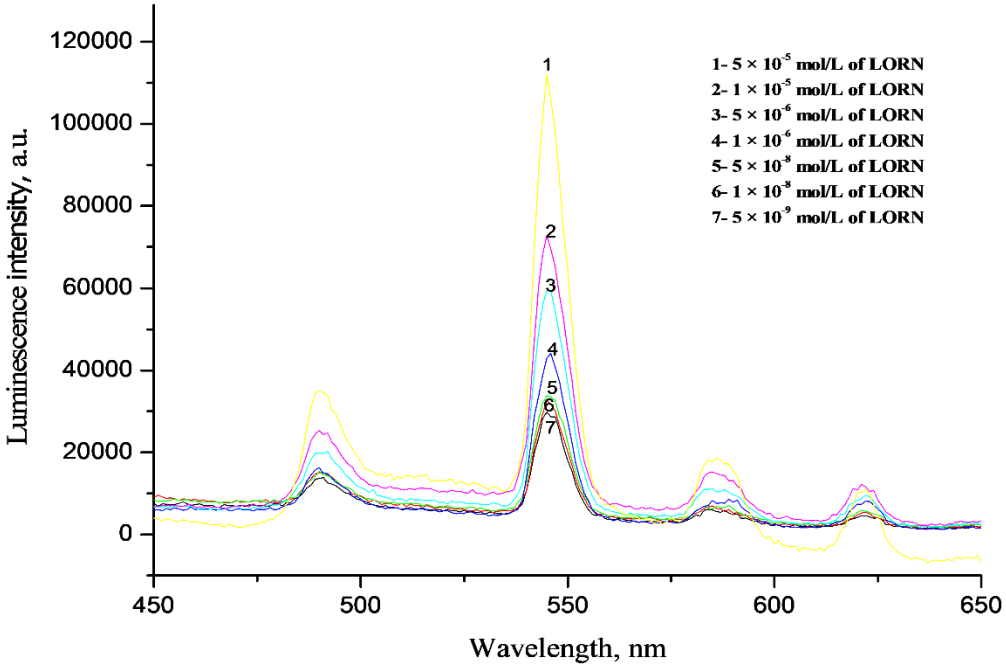


**Fig. 9.** Luminescence emission spectra of 3 x $10^{-4}$ mol/L $Tb^{3+}$ in presence of different concentrations of Lornoxicam in acetonitrile at pH=5.5.

### *8.2. Linear range and detection limit*

This investigation evaluated the influence of Lornoxicam concentration (from 5 × $10^{-9}$ to 5 × $10^{-5}$ mol/L) on the emission intensity of a novel photo probe, measured at 545 nm. The data, presented in Fig. (10), demonstrat a linear correlation defined by the equation Y = a + bX, where Y is the luminescence intensity and X is the concentration. The calibration parameters, detailed in Table (1), include an intercept (a) of 34269.31, a

slope (b) of 406.58 × $10^9$, and a strong correlation coefficient (R) of 0.99. Adhering to ICH criteria, the method's sensitivity was assessed by calculating the limit of detection (LOD) and limit of quantification (LOQ). These were derived from the formulas LOD = 3.3 S/b and LOQ = 10 S/b, where S represents the standard deviation of blank measurements (3.03 mol/L) **(ICH, 2003; ICH, 2005; Attia *et al.*, 2011d, e, 2014, 2016, 2019a, b, 2020; Abdullah & Attia, 2019)**. The resulting LOD was 2.45 × $10^{-11}$ mol/L, and the LOQ was 7.37 × $10^{-11}$ mol/L. The exceptionally low LOD, combined with the extensive linear working range, confirms the high sensitivity of this analytical approach.

**Table 1.** Sensitivity and regression parameters for photo probe

| Parameter | Values |
|---|---|
| $\lambda_{em}$, nm | 545 |
| Linear range, mol/L | 5 × $10^{-9}$ to 5 × $10^{-5}$ |
| Limit of detection (LOD), mol/L | 2.45 × $10^{-11}$ |
| Limit of quantification (LOQ), mol/L | 7.37 × $10^{-11}$ |
| Intercept | 34269.31 |
| Slope | 406.58 × $10^9$ |
| SD (S) | 3.03 |
| Variance ($S^2$) | 9.16 |
| Correlation coeffecient | 0.99 |

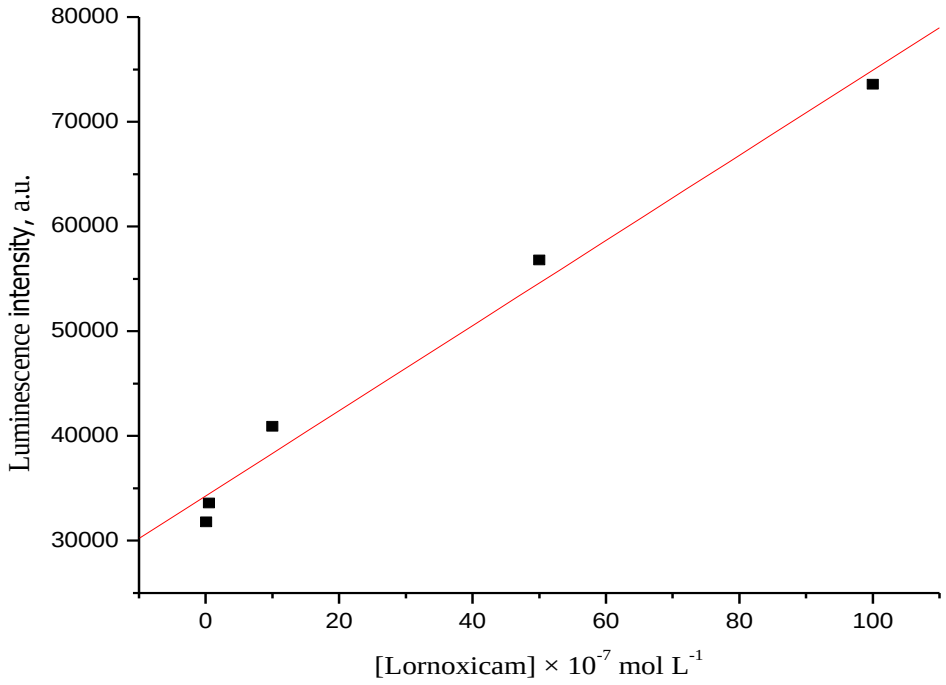


**Fig. 10.** Linear relationship between luminescence intensity of Lornoxicam -$Tb^{3+}$ complex at $\lambda_{em}$=545 nm and concentration of Lornoxicam

### *8.3. Precision and accuracy*

**Accuracy (Recovery %, Table 2)**

For the Nile River samples, the recovery percentages were 103.70 and 101.60%, indicating excellent accuracy. When the method was used to measure lornoxicam added to the complex river water matrix, it recovered almost all of the analyte, showing values very close to 100%. The slight values exceeding 100% are common in complex samples and are well within acceptable limits for environmental analysis, suggesting minimal interference from other substances present in the river water.

**Precision (RSD%)**

Intra-day precision (Repeatability): The RSD% for the Nile River samples was 0.90 and 3.70%. Although the 3.70% value for Sample 2 was slightly higher than ideal, it remained acceptable for environmental analysis and was comparable to or better than the standard method's RSD of 4.10%.

**Inter-day precision (Intermediate precision)**

The RSD% values were 1.80 and 3.20% for the two river samples. These results demonstrated that the method produced consistent outcomes not only within the same day but also across different days, which is crucial for long-term environmental monitoring.

**Comparison to standard method**

The proposed method's average readings were very close to those obtained using the standard method, often showing lower RSD% values. This confirmed that the new method was equally accurate but more reliable and precise.

**Table 2.** Evaluation of intra-day and inter-day precision for optical sensor $Tb^{3+}$-(Lornoxicam)

| Pharmaceutical formulation | Standard method | Proposed method | | | | | | Recovery % |
|---|---|---|---|---|---|---|---|---|
| | Average (conc) ± RSD% x $10^{-7}$ | Intraday precision | | | | Interday Precision | | |
| | | Average reading x $10^{-7}$ | RE % | RSD % | Average reading x $10^{-7}$ | RE % | RSD% | |
| Sample 1(Nile River) | 13.5 ± 3.9 | 13.59 | 0.66 | 0.90 | 14.0 | 3.70 | 1.80 | 103.70 |
| Sample 2 (Nile River) | 18.7 ± 4.1 | 18.78 | 042 | 3.7 | 19.0 | 1.61 | 3.20 | 101.60 |
| Lornoxicam (8 mg) | 10.1 ± 2.9 | 10.13 | 0.29 | 2.70 | 10.2 | 0.99 | 3.30 | 100.29 |
| | 1.015 ± 1.8 | 1.021 | 0.59 | 2.14 | 1.03 | 1.47 | 3.50 | 100.59 |

***8.4. Robustness and ruggedness***

**Robustness**

To assess the reliability of the photo probe method, researchers investigated its tolerance to various experimental changes. They incrementally modified the concentration of $Tb^{3+}$, pH, and contact time, observing minimal impact on the probe's

luminescence intensity. Robustness: The method was unaffected by small, deliberate changes in key parameters ($Tb^{3+}$ concentration, pH, interaction time). The %RSD values for these changes were exceptionally low (≤ 0.98%). This means that even if there are minor fluctuations during sample preparation or analysis (e.g., slight pH changes in the river water), the results will remain highly reliable.

**Ruggedness**

The method produced consistent results (RSD ≤ 1.08%) when the analysis was performed by three different analysts. This proves that the method is not operator-dependent and can be successfully transferred to other laboratories for routine monitoring of the Nile River or other water bodies.

**Table 3.** Method robustness and ruggedness expressed as intermediate precision (% RSD)

| Method | Average value<br>Standard method x $10^{-7}$ | Proposed method | | | |
|---|---|---|---|---|---|
| | | Robustness | | | Ruggedness |
| | | Parameter altered | | | Inter-analysts, (%RSD)<br>(n=3) |
| | | Concentration of $Tb^{3+}$ (%RSD) | pH change (%RSD) | Interaction time | |
| 1 | 10 | 0.58 | 0.98 | 0.11 | 1.01 |
| 2 | 1.0 | 0.88 | 0.78 | 0.12 | 1.08 |

**Application to pharmaceutical formulation and environmental samples**

The proposed method was successfully applied to determine Lornoxicam in both commercial pharmaceutical formulations and real-world environmental samples, demonstrating its versatility and reliability.

For the quality control of an 8 mg Lornoxicam vial, the method exhibited excellent accuracy and precision. The analysis yielded a mean concentration with a recovery of 100.29%, confirming excellent agreement with the labeled claim. The method's precision, expressed as a relative standard deviation (RSD), was 3.3%, which is

comparable to or better than the standard British Pharmacopoeia (BP) method (RSD of 3.5%). This validates the method as a precise and accurate alternative for routine pharmaceutical analysis.

Critically, the method proved highly effective for detecting Lornoxicam at trace levels in complex matrices, as demonstrated with wastewater from the Nile River. For two separate river water samples, the method achieved high accuracy with recoveries of 103.70 and 101.60%, indicating minimal matrix interference. The precision for these environmental samples was also satisfactory, with inter-day RSD values of 1.80 and 3.20%, respectively. This confirms the method's suitability for sensitive and reliable environmental monitoring of pharmaceutical pollutants.

## CONCLUSION

A unique photoprobe was developed for detecting lornoxicam (LORN), a drug used to treat pain and inflammation. This probe, composed of a terbium–lornoxicam (Tb–LORN) complex in acetonitrile at a pH of 5.5, offers several advantages. The method provides a superior approach for pharmaceutical quality control. It is sensitive, selective, robust, and cost-effective compared with existing methods for ensuring the correct dosage of lornoxicam in medicine vials.

Extended Application: The method’s high sensitivity also makes it a powerful tool for environmental science. The successful detection and quantification of lornoxicam in the Nile River water samples demonstrate its potential for monitoring pharmaceutical pollution in the environment, a growing global concern.

## REFERENCES

**Abdel-Mottaleb, M.S.A.; Saif, M.; Attia, M.S.; Abo-Aly, M.M. and Mobarez, S.N. (2018).** *Photochemical & Photobiological Sciences, 17,* 221–230.

**Abdullah, L.M. and Attia, M.S. (2019).** *Journal of Fluorescence, 29,* 247–255.

**AlGhamdi, H.A.; AlZahrani, Y.M.; Alharthi, S. and Attia, M.S. (2023).** *RSC Advances, 13,* 21769–21780.

**Attia, M.S. and Al-Radadi, N.S. (2016).** *Biosensors and Bioelectronics, 86,* 413–419.

**Attia, M.S.; Khalil, M.H.; Abdel-Mottaleb, M.S.A.; Lukyanova, M.B.; Alekseenko, Yu.A. and Lukyanov, B.S. (2006).** *International Journal of Photoenergy, 2006,* 1–9.

**Attia, M.S.; Bakir, E.; Abdel-Aziz, A.A. and Abdel-Mottaleb, M.S.A. (2011a).** *Talanta, 84,* 27–33.

**Attia, M.S.; Mahmoud, W.H.; Ramsis, M.N.; Khalil, L.H.; Othman, A.M.; Hashem, S.G. and Mostafa, M.S. (2011b).** *Journal of Fluorescence, 21,* 1739–1748.

**Attia, M.S.; Mahmoud, W.H.; Youssef, A.O. and Mostafa, M.S. (2011c).** *Journal of Fluorescence, 21,* 2229–2235.

**Attia, M.S.; Othman, A.M.; Elraghi, E. and Aboul-Enein, H.Y. (2011d).** *Journal of Fluorescence, 21,* 739–745.

**Attia, M.S.; Ramsis, M.N.; Khalil, L.H. and Hashem, S.G. (2012a).** *Journal of Fluorescence, 22,* 779–788.

**Attia, M.S.; Youssef, A.O. and Essawy, A.A. (2012b).** *Analytical Methods, 4,* 2323–2328.

**Attia, M.S.; Youssef, A.O.; Elgazawy, A.-S.S.H.; Agami, S.M. and Elewa, S.I. (2014).** *Journal of Fluorescence, 24,* 759–765.

**Attia, M.S.; Elsaadany, S.A.; Ahmed, K.A.; El-Molla, M.M. and Abdel-Mottaleb, M.S.A. (2015).** *Journal of Fluorescence, 25,* 119–125.

**Attia, M.S.; Youssef, A.O.; Khan, Z.A. and Abou-Omar, M.N. (2018).** *Talanta, 186,* 36–43.

**Attia, M.S.; Ali, K.; El-Kemary, M. and Darwish, W.M. (2019).** *Talanta, 201,* 185–193.

**Attia, M.S.; Mohamed, A.A.; El-Saady, M.M.; Abou-Omar, M.N.; Afify, H.G.; Amin, T.A.; Hosny, A.H.; Youssef, A.O. and Mohy-Eldin, M.S. (2022).** *Journal of Materials Chemistry C, 10,* 6464–6472.

**Balfour, J.A.; Fitton, A. and Barradell, L.B. (1996).** *Drugs, 51,* 639–657.

**Belal, F.; Omar, M.A.; Derayea, S.M.; Zayed, S.; Hammad, M.A.; Saleh, S.F.; Alhazmi, H.A. and Al Bratty, M. (2020).** *Current Pharmaceutical Analysis, 16,* 1148–1156.

**Bozal, B. and Uslu, B. (2010).** *Combinatorial Chemistry & High Throughput Screening, 13,* 599–609.

**Chaplenko, A.; Monogarova, O. and Oskolok, K. (2018).** *International Journal of Pharmaceutical and Biological Archive, 9,* 31–35.

**Elabd, A.A. and Attia, M.S. (2016).** *Journal of Luminescence, 169,* 313–318.

**Escudero, A. et al. (2017).** *Nanophotonics, 6,* 881–921.

**Ghoneim, M.; Beltagi, A. and Radi, A. (2002).** *Analytical Sciences, 18,* 183–186.

**Hanaoka, K.; Kikuchi, K.; Kobayashi, S. and Nagano, T. (2007).** *Journal of the American Chemical Society, 129,* 13502–13509.

**Hashem, S.G.; Elsaady, M.M.; Afify, H.G.; Omer, W.E.; Youssef, A.O.; El-Kemary, M. and Attia, M.S. (2019).** *Talanta, 199,* 89–96.

**International Conference on Harmonisation (ICH). (2003).** *Stability Testing of New Drug Substances and Products, Q1A(R2).*

**International Conference on Harmonisation (ICH). (2005).** *Validation of Analytical Procedures: Text and Methodology, Q2(R1).*

**Lee, S.Y.; Lin, M.; Lee, A. and Park, Y.I. (2017).** *Nanomaterials, 7,* 411.

**Mettam, G.R.; Daly, G.; Khalil, T. and Adams, L.B. (2009).** Introduction to the Electronic Age. In: *E-Publishing Innovations;* Jones, B.S. and Smith, R.Z., Eds.; E-Publishing Inc.: New York, pp 281–304.

**Omer, W.E.; El-Kemary, M.A.; Elsaady, M.M. and Attia, M.S. (2020).** *ACS Omega, 5,* 5629–5637.

**Sahoo, S.K.; Giri, R.K.; Patil, S.V.; Behera, A.R. and Mohapatra, R. (2012).** *Tropical Journal of Pharmaceutical Research, 11,* 269–273.

**Salunkhe, N.; Jadhav, N. and Bhinge, S. (2019).** *Separation Science Plus, 2,* 405–415.

**Shah, S.N.H.; Sohail, K.; Javaid, Z.; Zaman, M. and Basheer, E. (2019).** *Pakistan Journal of Pharmaceutical Sciences, 32,* 333–338.

**Taha, E.A.; Salama, N.N. and Fattah, L.E.-S.A. (2006).** *Chemical & Pharmaceutical Bulletin, 54,* 653–658.

**Weibel, N.; Charbonniere, L.J.; Guardigli, M.; Roda, A. and Ziessel, R. (2004).** *Journal of the American Chemical Society, 126,* 4888–4896.

**Younis, H.M.; Youssef, A.O.; El-Sheikh, S.M.; Sheta, S.M. and Attia, M.S. (2023).** *Microchemical Journal, 194,* 109297.

**Zhang, N.; Tang, S.-H. and Liu, Y. (2003).** *Spectrochimica Acta, Part A: Molecular and Biomolecular Spectroscopy, 59,* 1107–1112.